

## DYNAMIC BEHAVIOUR OF HIGH MANGANESE STEELS

JABŁOŃSKA Magdalena Barbara

*Silesian University of Technology, Katowice, Poland, EU*

[magdalena.jablonska@polsl.pl](mailto:magdalenajablonska@polsl.pl)

### Abstract

High strength properties and a wide range of deformation hardening, particularly in case of dynamic deformation, enable application of manganese steels in the structure of highly strained elements constituting mechanical vehicle framework. This is true primarily for railway, automotive and military industries, where not only decrease in weight, but also safety improvements are of importance. Favourable combination of strength and ductility, as well as excellent ability to absorb energy in the deformation process which is a characteristic of those steels allow the assumption that the possibilities of their usage in the structures of means of transport will become more and more common, and that the demand for materials of that kind will be growing along with the sharpening of structure regulations and bump test norms. Mechanical properties together with mass density higher than in traditional types of steel constitute a new quality of steel structure materials designed for those industries. Manganese steels are characterized by their ability to activate distinct deformation mechanisms, such as twinning induced by plastic deformation, that is referred to in technical literature as the TWIP effect (twinning-induced plasticity), as well as MBIP (microband-induced plasticity), that are responsible for the combination of high strength and ductility in steels to be examined and consequently, for high energy absorption, a basic control parameter in crush tests carried out on vehicles. The aim of this research is to explain of structural phenomena that take place during mechanical twinning induced as well as formation deformation microbands in austenitic matrix by dynamic plastic deformation in steels with the TWIP effect. This research focuses on the analysis of structure changes taking place in manganese steels depending on the stacking-fault energy (SFE) affected by chemical composition, and on the applied variable plastic deformation rate. The conducted research will generate data for the model description of structure changes under the influence of varying deformation rate that take place in manganese steels of different SFE value.

**Keywords:** Manganese steels, TWIP effect, dynamic deformation, microstructures

### 1. INTRODUCTION

Current needs of the most important branches of economy, such as, for instance, automotive and railway industries, are connected with manufacturing of new materials with significantly more favourable set of mechanical and plastic properties, and taking the economic aspects under consideration. Pursuit of reduction in vehicle mass results in application of various material groups such as composites, polymers or light alloy materials, but the most important elements with the highest degree of responsibility for safety are still manufactured from steels. However, the approach to designing modern steels with a broad range of strength and plastic properties is changing fundamentally [1-5]. Among these steels, one may include steels from the group reinforced in the result of structural effects induced by plastic deformation. Particularly selected groups of Advanced High Strength Steels (AHSS) with manganese exhibiting characteristic effects during deformation, i.e. the ones caused by hardening by mechanical twinning of the austenite, the so-called TWIP effect (twinning induced plasticity), and hardening by formation of shear microbands in the austenite, the so-called MBIP effect (microbands induced plasticity) **Figure 1**, belong to them [1, 7-10]. Both these effects influence uniquely the combination of mechanical and plastic properties, and their occurrence depends on the

criterion of selection of chemical composition, and therefore control of stacking fault energy  $\gamma$  SFE. The details of the mechanisms controlling strain-hardening in high manganese steels are still unclear [2,7,8-14].

### New Generation Manganese Steels

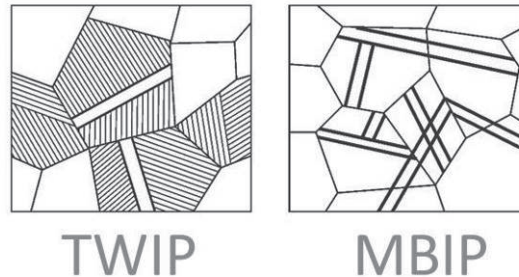


**Figure 1** New-generation groups of AHSS manganese steels with a schematic presentation of the main mechanism of their hardening (developed based on [2-5, 9]): a) hardening by mechanical twinning, b) hardening by formation of shear microbands

SFE value is the measure of tendency to twinning induced deformation. and is in manganese steels in the range of  $20 \text{ mJ} / \text{m}^2$  to  $60 \text{ mJ} / \text{m}^2$ . For SFE above  $60 \text{ mJ} / \text{m}^2$  steels tend to develop microbands [17, 19, 22, 23]. The value of stacking fault energy is controlled by contents of alloying elements, so the variable is the value of  $\Delta G^{\gamma \rightarrow \epsilon}$  being a difference of molar Gibbs free energy between austenite and martensite phases in relation to the individual alloying elements. The fundamental alloying component controlling stability of austenite during deformation of the discussed steels is manganese. Increasing its contents initially leads to a decrease in SFE to a minimum value below  $5 \text{ mJ} / \text{m}^2$ , and then increases again. Simultaneously at this Mn contents, introduction of Al to the steel generates an increase in SFE and effectively limits the deformation-induced  $\gamma \rightarrow \epsilon \rightarrow \alpha$  transformation, stabilizing high-manganese austenite, what also favours deformational hardening in a result of TWIP and MBIP effects [5, 6 8 - 14]. The SFE value depends not only on the chemical composition, but also on the deformation temperature. Correlation of these two factors directly determines the dominant deformation mechanism, especially in relation to manganese steel [2]. As temperature increases, thermal activation facilitates slip dislocation, inhibiting the growth of deformation twins [24]. However, it has been shown that up to about  $300^\circ \text{C}$  the tested TWIP steels still have an EBU of between  $20 \text{ mJ} / \text{m}^2$  and  $60 \text{ mJ} / \text{m}^2$ . Therefore, the effect of temperature on changing EBU should only be considered at temperatures above  $300^\circ \text{C}$ . It is characteristic that manganese steels, especially TWIP, have a strong relationship between properties and deformation rate [21-27]. They show the ability to be strengthened with the increase in deformation rate without loss of good plastic properties. Contrary to the increasing number of publications on the properties of manganese steel deformed under high speed conditions, little is known about the structural changes that accompany this process. Part of the work also applies only to deformation in cold or hot working processes [10, 11, 17, 19]. Only in a few works can you find reports on the structure of Mn-Al steels, including TWIP and its changes analyzed by LM and TEM techniques under deformation at high strain rates. In the paper several properties of manganese TWIP steel as well as the microstructure analysis after static and dynamic deformation was performed.

## 2. EXPERIMENTAL PROCEDURE

A manganese steel Fe - 26 wt.% Mn - 5 wt.% Al - 5 wt.% Si - 0.6 wt.% C, was the material for studies. The steel was smelted in a vacuum induction furnace with a ceramic melting pot, and cast using gravity casting technique. The obtained ingots were forged into round bars with a diameter of 20 mm. The forging was carried out so as to the forging start temperature was in the range of  $1150^\circ \text{C} \pm 1140^\circ \text{C}$ , and the forging finish temperature was not lower than  $900^\circ \text{C}$ . After the forging, the bars were subjected to hyperquenching from a

temperature of 1170°C. In this material state, the studied steel had a monophasic austenitic structure with characteristic annealing twins, with a hardness 185 HV2. The static tensile tests were carried out at standard ZWICK machine with a maximum force of 250 kN. The series of measurements was made according to PN-EN ISO 6892-1: 2010 [28]. Round specimens with a diameter of 4 mm, ending with threaded M10 heads, were used. A measuring base of 20 mm length was used for measuring the elongation  $A_5$ . The strength and geometry of the sample before and after the deformation were determined by the following: tensile strength TS, yield strength YS, elongation  $A_5$ . The dynamic tensile tests were carried out on a flywheel machine of RSO type, owned by Institute of Materials Technology of Silesian University of Technology, with an impact linear velocity in the range of 5÷40 m/s, corresponding to deformation rates in the range of  $10^2$ ÷ $10^4$  s<sup>-1</sup>. During the dynamic tensile tests, the sample is connected to the top holder, and it is deformed by an impact of a ram into the anvil of the bottom holder. The ram linear velocity was determined by a measurement of the rotational speed of the ram's flywheel. Smooth cylindrical samples with a diameter of 4 mm and a measurement part length of 20 mm were used for the tests, bilaterally threaded in the holder part. During the tests, the course of the tensile force vs. time, and the linear velocity of the ram placed in the flywheel, were recorded. Based on the force characteristics and sample geometry measurements before and after the deformation, the following parameters were determined: limiting deformation  $\epsilon_g$ , deformation rate, tensile strength TS. The structural studies were carried out by optical light microscopy and in the submicroscopic scale, using transmission scanning electron microscopy. The hardness measurement was carried out by Vickers method under a load of 2 kg.

### 3. RESULTS AND ITS DISCUSSION

The results of the static tensile test are shown in **Table 1**. The YS of the deformation steel at 0.0005 s<sup>-1</sup> is 680 MPa and decreases to 630 MPa for deformation at a rate of 0.01 s<sup>-1</sup>. Steel reaches TS, 915 MPa for deformation at 0.0005 s<sup>-1</sup> and 820 MPa for deformation at 0.01 s<sup>-1</sup>. Good plasticity properties were achieved, elongation of  $A_5$  was 40%. For the 0.0005 s<sup>-1</sup> deformation rate YS / TS yield index reaches 0.74 and the deformation rate 0.01 s<sup>-1</sup> is 0.73.

**Table 1** Results obtained in static tensile test of steel.

Strain rate, s <sup>-1</sup>	TS	YS	$A_5$ , %	YS/TS
0.0005	915	680	41	0.74
0.01	820	630	40	0.73

Dynamic deformation tests using flywheel machine were carried out with the ram's linear velocity of 15, and 30 m/s. It corresponds to obtained deformation rates in the range of 100÷4000 s<sup>-1</sup>. The calculated value of the deformation limit  $\epsilon_g$  increases as the steel deformation rate increases during dynamic tests (**Table 2**). The tested steel achieves high values of the deformation limit. For deformation rate 1830 s<sup>-1</sup>, the  $\epsilon_g$  is 0.94, while for the deformation rate 4650 s<sup>-1</sup> the value of  $\epsilon_g$  is 1.30. Such characteristics indicate that the material is characterized by very high plasticity at deformation at very high speeds. The studied steel exhibits sensitivity of the stress to the deformation rate. Values of the TS determined after dynamic tests are gathered together with the TS value after the static tensile test. The investigations indicate that an increase in the deformation rate is accompanied by an increase in the tensile strength. In the static tensile test, the average value of TS amounts to 870 MPa, while after the dynamic tensile test, this values increases almost twice, reaching averages of 1517 MPa and 1633 MPa, for the ram's linear velocities of 15 m/s and 30 m/s, respectively. At the highest ram's linear velocity used, i.e. 30 m/s, the studied steel exhibits the highest tensile strength. The studied steel is being strongly hardened, what is confirmed by the results of the hardness test. Measurement of hardness was done on longitudinal elimination with a 0.35 mm step on a 15 mm<sup>2</sup> surface. Measurements were made at a distance of 0.5 mm from the edges of the sample. Hardness measurement values averaged for each deformation variant (**Table 3**) indicate an increase in the hardness of the steel under test due to the

increase in deformation rate, with the highest increase in hardness HV2 occurring at the transition from the static to the dynamic range.

**Table 2** Results obtained in dynamic tensile test of steel.

Strain rate, s <sup>-1</sup>	Linear velocity, m/s	TS	ε <sub>g</sub>
1580	15	1545	0.87
1830	15	1490	0.94
4190	30	1650	1.15
4650	30	1615	1.30

**Table 3** Results of hardness HV2 after static and dynamic tensile test of steel.

Strain rate, s <sup>-1</sup>	HV2
initial state	185
0.0005	360
0.01	340
1830	380
4650	401

On the base of dynamic tests results according to formula (1) as the integral represents the field of the tensile graph between the curve, the abscissa and the end of the graph we obtain the value of deformation work. Follow then we calculated the energy absorption during the deformation process according to formula (2). [29 - 31]

$$L_u = \int_0^{\Delta l} F d(\Delta l) = \int_{l_0}^{l_1} F \cdot dl, J \quad (1)$$

$$E_{ABS} = \frac{L_u}{V}, J / mm^3 \quad (2)$$

where :  $L_u$  - deformation work, J;

$V_S$  - volume of measuring base, mm<sup>3</sup>

The calculated value of the plastic deformation  $L_u$  required to break the specimen in the tensile test on the flywheel machine is 4650 s<sup>-1</sup> 106.5 J. The results calculated for the series of samples are shown in **Table 4**. It can be seen that the increase in the deformation rate of the test steel affects the increase in the value of deformation work required to destroy a sample in dynamic tests. The value of the absorbed energy of the deformation, ie the  $E_{ABS}$ , was determined by the plastic deformation measured in relation to the sample volume [29-31].

**Table 4** Results of calculated  $L_u$  and  $E_{ABS}$  after dynamic tensile test of steel.

Strain rate, s <sup>-1</sup>	$L_u$ , J	$E_{ABS}$ , J/mm <sup>3</sup>
1830	77	0.30
4650	114	0.47

The results show that the steel exhibits the highest energy absorption capacity at stretching speed of 4650 s<sup>-1</sup> and is 0.47 J / mm<sup>3</sup>. The structure of the tested steel after static and dynamic tensile reveals the effects of cold plastic deformation in the form of austenite grains inside which mechanical twists and deformation bands

occur (**Figure 2**). An increase in defected caused by the increase in deformation rate is observed. After deformation in static conditions (**Figure 3a**) highly defected areas dominate the structure. On the background of the cellular dislocation structure there are single mechanical twins and microbands. Twins deformation occur in one twin system. The cellular structure borders on areas of high defected of austenite. Deformation at dynamic conditions **Figures 3b, c**) favors the formation of a cellular dislocation structure. Usually dislocation cells are poorly formed and austenite areas are characterized by very high degradation. There are also selected areas of well-developed dislocation cells (under the highest strain rate conditions) and occupy most of the austenitic matrix. The twinning process is activated and predominantly two primary and secondary systems are active. Twins of deformation are visible in the form of bands of varying widths. The distinctive deflections of the twins of deformation, resulting from the high activity of the twinning system, are noticeable. The microbands are visible as the effect of deformation.

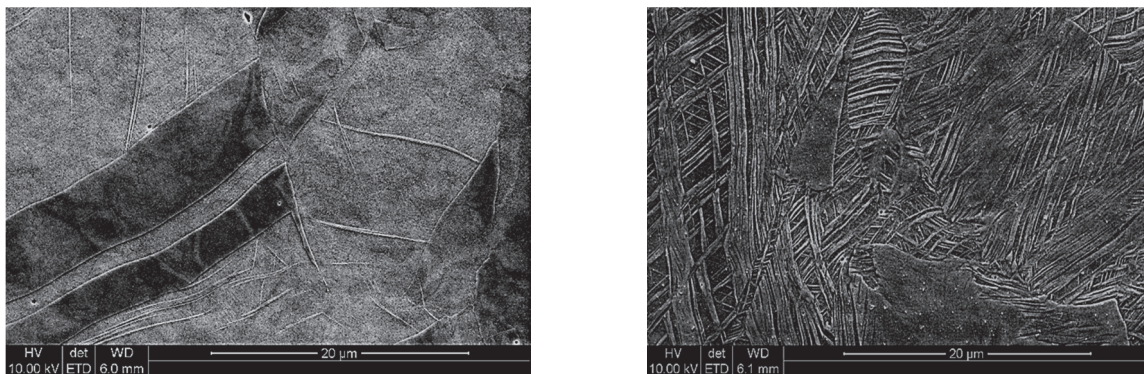


**Figure 2** Microstructure of steel after a) static tensile, b) dynamic tensile, SEM, visible defected austenite structure by creation of mechanical twins and microbands

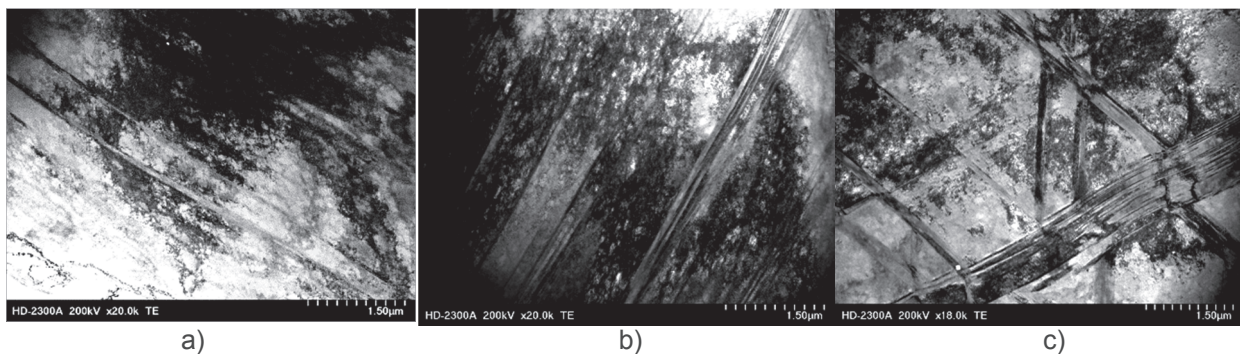


**Figure 3** Microstructure of steel after a) static tensile, b, c) dynamic tensile, STEM, visible defected austenite structure by creation of mechanical twins and microbands.

The high deformation rates initiates the processes of intense mechanical twinning. Against the backdrop of the dislocation structure that undergoes transformation, the twin systems of deformation develop in two systems.

#### 4. CONCLUSION

In literature, there is little work in which the changes of the microstructure of high-manganese steel strengthened by mechanical twinning occur under different cold deformation rates. The results obtained and presented here are a new concept. The use of static and dynamic tensile methods has allowed the material characteristics to be obtained over a wide range of steel deformation rates. The dynamic test confirmed that the TS of the steel is sensitive to the deformation rate. Under tensile conditions at the maximum strain rate,

the steel is characterized by high plasticity. It was calculated that the steel is characterized by high  $E_{ABS}$  value. It confirms the ability to capacity dynamic loads. Under static tensile conditions, the dislocation slip plays a dominant role in the deformation of steel. Under the dynamic conditions, the share of the twinning mechanism in the steel deformation increases. Twins are most often formed in two systems, and the process of generating mechanical twins is accompanied by the effects of dislocation slip. There is a continuous transformation of the dislocation structure as a result of increasing deformation.

## ACKNOWLEDGEMENTS

*The work was supported by the Ministry of Science and Higher Education  
within the framework of the BK-225/RM0/2017*

## REFERENCES

- [1] WEI Y., LI Y., ZHU L., LIU YAO, LEI X., WANG G., WU Y., MI Z., LIU J., WANG H. & GAO H.: Evading the strength-ductility trade-off dilemma in steel through gradient hierarchical nanotwins, *Nature Communications*, 2014, p. 1-8.
- [2] BOUAZIZ O., ALLAIN S., SCCOT C.P, CUGY P., BARBIER D.: High manganese austenitic twinning induced plasticity steels: A review of the microstructure properties relationships, *Opinion in Solid State and Materials Science*, Vol. 15, 2011, p. 141-168.
- [3] HAMADA S.A.: Manufacturing, mechanical properties and corrosion behavior of high Mn TWIP steels, Ed. Oulu University Press, *Acta Universitatis Ouluensis C281*, 2007.
- [4] Advanced High-Strength Steels, Application Guidelines Ver. 5.0, World Auto Steel, 2014.
- [5] GRASSEL O., KRUGER L., FROMMEYER G., MEYER L.W.: High strength Fe-Mn-(Al, Si) TRIP/ TWIP steel development - properties - application, *International Journal of Plasticity* 16, 2000, p. 1391-1409.
- [6] RAABE D., SPRINGER H., GUTIERREZ-URRUTIA I., ROTERS F., BAUSCH M., SEOL J.-B., KOYAMA M., CHOI P.-P., TSUZAKI K.: Alloy Design, Combinatorial Synthesis, and Microstructure -Property Relations for Low-Density Fe-Mn-Al-C Austenitic Steels, *JOM*, Vol. 66, No. 9, 2014, p. 1845-1856.
- [7] KUZIAK R., KAWALLA R., WAENGLER S.: Advanced high strength steels for automotive industry, *Archives of Civil and Mechanical Engineering* 8, 2008, p. 103-117.
- [8] YOO J.D., PARK K.T.: Microband-induced plasticity in a high Mn-Al-C light steel. *Materials Science and Engineering* 496A, 2008, p. 417-424.
- [9] KIM H., SUH D., KIM N.: Fe-Al-Mn-C light weight structural alloys: a review on the microstructures and mechanical properties, *Science and Technology of Advanced Materials* 4, 2013, p. 1-11.
- [10] KOZŁOWSKA a. GRAJCAR A.: Effect of chemical composition and plastic deformation on corrosion properties of highMn austenitic steels in alkaline solution, *Archives of Materials Science and Engineering*, 2016, 77, P. 31-39
- [11] BLECK W.: Effect of Microalloying in Multi Phase Steels fo Car Body Manufacturing, *Materiały konferencji "14 Sächsische Fachtagung Umfortechnik"*, Freiberg, 2007
- [12] PECNIK C.M., RECHBERGER F., HÄNZI A.C., LÖFFLER J.G F., UGGOWITZER P.J. , Recrystallization behavior, microstructure evolution and mechanical properties of biodegradable Fe-Mn-C(-Pd) TWIP alloys, *Acta Materialia*, Volume 60, Issues 6-7, April 2012, pp. 2746-2756
- [13] GUTIERREZ-URRUTIA I., ZAEFFERER S., RAABE D., The effect of grain size and grain orientation on deformation twinning in a Fe-22 wt.% Mn-0.6 wt.% C TWIP steel, *Materials Science and Engineering*, A 527, 2010,p. 3552-3560.
- [14] JABŁOŃSKA M.B., ŚMIGLEWICZ A., NIEWIELSKI G. The effect of strain rate on the mechanical properties and microstructure of the high-mn steel after dynamic deformation tests, *Archives of Metallurgy and Materials*, 2015, 60, 2, pp. 577-580.
- [15] FROMMEYER G., BRÜX U.: Microstructures and mechanical properties of high-strenght FeMn-Al-C Light TRIPLEX Steels, *Steel Research International*, vol. 77, 2006, s.627633.
- [16] SATO K., ICHINDOSE M. HIROTSU Y.: Effects of deformation induced phase transformation and twinning on the mechanical properties of austenitic Fe-Mn-Al alloys, *ISIJ International*, vol. 29., No 10, 1989, p. 868-877.

- [17] JABŁOŃSKA M.B.: Mechanical properties and fractographic analysis of high manganese steels after dynamic deformation tests, *Archives of Metallurgy and Materials*, 2014, 59, 3, pp. 1193-1197.
- [18] GRAJCAR A, WOŹNIAK D, KOZŁOWSKA A, Non-Metallic Inclusions and Hot-Working Behaviour of Advanced High-Strength Medium-Mn Steels, *Archives of Metallurgy and Materials*, 2016, 61 (2), p. 811-820.
- [19] JABŁOŃSKA M, ŚMIGLEWICZ A: A study of mechanical properties of high manganese steels after different rolling conditions, 2016, *Metalurgija* 54 (4), 619-622
- [20] FROMMEYER G., BRUX U., NEUMANN P.: Supra-ductile and high-strength manganese-TRIP/TWIP steels for high energy absorption purposes, *ISI International* 43, 2003, pp. 438-446.
- [21] ŚMIGLEWICZ A, MOĆKO W, RODAK K, BEDNARCZYK I, JABŁOŃSKA MB: Study of Dislocation Substructures in High-Mn Steels after Dynamic Deformation Tests, *Acta Physica Polonica A*, 2016, 130 (4), pp. 942-945.
- [22] DUMAY A., CHATEAU J.-P., ALLAIN S., MIGOT S., BOUAZIZ O.: Influence of addition elements on the stacking-fault energy and mechanical properties of an austenitic Fe-Mn-C steel, *Materials Science and Engineering A* 483-484, 2008, p. 184-187.
- [23] KIM J., LEE S.J., DE COOMAN B.C.: Effect of Al on the stacking fault energy of Fe-18Mn-0.6C twinning-induced plasticity, *Scripta Materialia* 65, 2011, p. 363-366.
- [24] ALBOU A., GALCERAN M., RENARD B K., GODETB A S., JACQUESA P.J. Nanoscale characterization of the evolution of the twin-matrix orientation in Fe-Mn-C twinning-induced plasticity steel by means of transmission electron microscopy orientation mapping, *Scripta Materialia*, 2013. 68, pp. 400-403.
- [25] MOĆKO W., KRUSZKA L.: Results of strain rate and temperature on mechanical properties of selected structural steels, *Procedia Engineering* 57, 2013, pp. 789-797.
- [26] CURTZE S., KUOKKALA V.T.: Effects of temperature and strain rate on the tensile properties of TWIP steels, *Revista Materia* 2, 2010, pp. 157-163.
- [27] SAHU P., CURTZE S., DAS A., MAHATO B., KUOKKALA V.T., CHOWDHURY S.G.: Stability of austenite and quasi-adiabatic heating during high strain-rate deformation of twinning-induced plasticity steels, *Scripta Materialia* 62, 2010, pp. 5-8.
- [28] PN-EN ISO 6892-1:2010: Metale i stopy metali - Próba statycznego rozciągania przy obciążeniu do 250 kN w temperaturze otoczenia, PL.
- [29] NIECHAJOWICZ A., TOBOTA A.: Application of flywheel machine for sheet metal dynamic tensile tests, *Archives of Civil and Mechanical Engineering* 8, 2008, pp. 129-137.
- [30] PŁACHTA A., PAWLICKI J., RODAK K.: Strength-energy and structural effects of dynamic deformation of aluminum alloy, *Solid State Phenomena* 226, 2015, pp. 49-52.
- [31] FROUSTEY C., LAMBERT M., CHARLES J.L., LATAILLADE J.L.: Design of an impact loading machine based on a flywheel device: application to the fatigue resistance of the high rate pre-straining sensitivity of aluminum alloys, *Experimental Mechanics* 47, 2007, pp. 709-721.